Synthesis and Characterization of sPS/Montmorillonite Nanocomposites

L. Torre, G. Lelli, J. M. Kenny

Materials Engineering Centre, University of Perugia, Loc. Pentima Bassa 2105100 Terni, Italy

Received 12 July 2005; accepted 3 October 2005
DOI 10.1002/app.23803
Published online in Wiley InterScience (www.interscience.wiley.com).

ABSTRACT: The present work analyzed the possibility of obtaining and producing syndiotactic polystyrene (sPS)–based nanocomposites. The work first focused on possible technology to use for intercalation from solution and melt intercalation. Using a blend of sPS with atactic polystyrene (aPS) as the matrix was also considered. Thermal analysis techniques, such as differential scanning calorimetry (DSC) and thermogravimetry (TGA), were used to study the thermal properties and stability of the nanocomposites obtained and to select the most appropriate nanocharges. The effect of the introduction of nanofillers on these properties also was evaluated. X–ray diffraction was used to investigate the degree of clay exfoliation. Finally, mechanical characterization of the nanocomposites obtained was performed and compared to that of the pure material. The tests demonstrated that nanodispersion of phyllosilicate layers improved the mechanical behavior of the polymers analyzed, especially the annealed sPS. © 2006 Wiley Periodicals, Inc. J Appl Polym Sci 100: 4957–4963, 2006

Key words: polystyrene; nanocomposites; clay; differential scanning calorimetry (DSC); thermogravimetric analysis (TGA)

INTRODUCTION

The possibility of industrially exploiting the capacity of clay to be dispersed on a nanometer scale in a polymer matrix has been extensively investigated since the early 1990s, when Toyota researchers announced the synthesis of a montmorillonite/nylon 6 nanocomposite, in which polymer performance was noticeably improved by the synergy with the nanoreinforcement.[1]

Since then, several polymer/clay combinations have been analyzed. Only some of these formulations led to fully exfoliated (also known as delaminated) nanocomposites, that is, to nanoscaled hybrids characterized by the largest contact area between polymer and clay platelets. In fact, depending on how compatible the organo–modified phyllosilicate and the polymer matrix are, it is also possible to obtain either a microcomposite (with the clay acting as a distinct phase) or a merely intercalated structure (with the organic macromolecules not sufficiently penetrating the clay galleries to destroy the original stacking of the platelets).[2]

Correspondence to: L. Torre (torrel@unipg.it).

Contract grant sponsor: Italian Ministry of Education (MIUR) through Progetti di Ricerca di Interesse Nazionale (PRIN).

Syndiotactic polystyrene (sPS) is a very promising engineering polymer. It is synthesized with a specific metallocene catalyst, which enables a merely 100% stereo–regular conformation (having the phenyl rings regularly alternated from side to side with respect to the polymer chain backbone)[3] to be achieved. This opens the possibility of obtaining a semicrystalline arrangement. In contrast, atactic polystyrene (aPS) is characterized by a completely amorphous microstructure.[4] For this reason, sPS has the optimal combination of applicative properties, such as high melting point (about 270°C), good thermal and dimensional stability, low dielectric constant, low gas permeability, good chemical resistance, and remarkable mechanical properties; furthermore, its manufacture is not too expensive.[5,6]

Unfortunately, the intrinsic brittleness of this polymer has hindered its use. Thus far, this problem has been overcome by making blends with elastomers or by adding toughening additives, worsening the versatility of the resulting material. In this context, an interesting possibility is presented by the production of organoclay/sPS nanocomposites, as the presence of intercalated or fully exfoliated nanoreinforcement could toughen the polymeric matrix without worsening other properties.[7]

The aim of this work was to thoroughly investigate the effects of dispersed nanoclay (Cloisite®) particles on the processability and the mechanical behavior of syndiotactic polystyrene. In particular, X–ray diffraction was used to analyze the intercalation of the poly-

TABLE I
Chemical Structures of Organo-Modifiers used in Cloisite 15A and 20A clays

Material	Organo-modifier
Cloisite® 15A	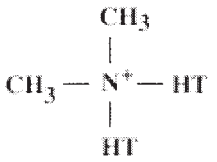 Modifier concentration: 125 meq/100 g clay
Cloisite® 20A	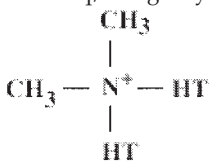 Modifier concentration: 95 meq/100 g clay

HT is hydrogenated tallow (~65% C18; ~30% C16; ~5% C14). Source: Southern Clay Products, Inc.

mer within the clay platelets. Thermogravimetric analysis (TGA) was conducted to evaluate the thermal stability of both nanoreinforcement alone and PS–based nanocomposites. In addition, both dynamic and isothermal differential scanning calorimetry (DSC) analyses were performed to examine the effect of the nanofiller on the thermal properties and the crystallinity of the nanocomposites.

Finally, it must be emphasized that the formation process is a key factor in achieving complete exfoliation. Several techniques for the production of sPS-based nanocomposites have been reported,[2–6,8] but the melt intercalation and solvent intercalation techniques seemed the most promising and therefore were used to synthesize the materials analyzed in the present study.

EXPERIMENTAL

sPS supplied by Dow Chemicals and aPS supplied by EniChem were used as polymeric matrices, to which 5 wt % of an organo-modified phyllosilicate was added as nanoreinforcement. Two modified montmorillonites (supplied by Southern Clay Products, Inc., Gonzalez, TX) were studied: Cloisite® 15A (MMT modified by dimethyl-dihydrogenated tallow–quaternary ammonium cation; modifier concentration: 125 meq/100 g clay) and Cloisite® 20A (MMT modified by dimethyl-dihydrogenated tallow–quaternary ammonium cation; modifier concentration: 95 meq/100 g clay). The chemical structures of the organo-modifiers are presented in Table I. The choice of organo-modifiers was grounded in the considerations of the compatibility of the selected polymer matrices with the organic part of the nanofillers (more information is provided in the Cloisite® selection chart, at the Southern Clay Products Web site, http://www.nanoclay-.com/c/c.html)[9].

It was previously decided to use the intercalation from solution method.[4,10,11] This method consists of forming a nanocomposite film by solvent evaporation, followed by hot pressing to produce the desired shape of the nanocomposite. There were several reasons for choosing this method, including that it made possible the use of material in small amounts and that better clay dispersion in the polymer would be obtained. Atactic polystyrene, because of its amorphous structure, easily dissolves in weak solvents like toluene. Therefore, aPS-based nanocomposites were prepared using a two-step process: first, the nanopowder was dispersed in toluene through sonication treatment (for 3 h at 80°C); then the polymer was added and sonication continued under the same conditions for about 5 h in order to obtain a homogeneous blend.

As syndiotactic polystyrene is highly resistant to solvents (even to aggressive liquids like 1,2-dichlorobenzene), it was necessary to adopt the melt intercalation method[5,6,10–14] in order to prepare sPS-based nanocomposites. The nanocomposites were prepared by mixing sPS with Cloisite® in a Bausano MD30 twin-screw extruder (with a temperature profile ranging from 250°C to 290°C) at the maximum extrusion speed (90 rpm). The extrusion process must be as fast as possible in order to prevent the thermal degradation of the nanoreinforcement (i.e., extrusion time should be very short relative to degradation onset time). Blends of aPS/sPS/Cloisite® (weight proportions: 47.5:47.5:5) also were prepared by melt intercalation.

Thermogravimetric analysis (TGA) was performed both in nitrogen and air atmospheres using a Seiko Instruments Exstar 6000. The scanning rate was 10°C/min, unless stated otherwise. Differential scanning calorimetry (DSC) was performed using a Mettler DSC822e/400 in a temperature range of 30°C–300°C at a heating and cooling rate of 10°C/min. To eliminate the influence of thermal history, the data from the first heating and cooling cycles were discarded for any analyzed material. Wide-angle X-ray scattering tests were performed using a CuKα (λ = 1.5428 Å) apparatus.

Finally, mechanical (tensile) tests were performed on a Lloyd Instruments LK30 universal dynamometer.

RESULTS AND DISCUSSION

Thermogravimetric analysis

To select the most appropriate nanofiller for all the types of polystyrene considered, it was necessary to perform a TGA analysis, mainly because of the relatively high processing temperatures of aPS and the

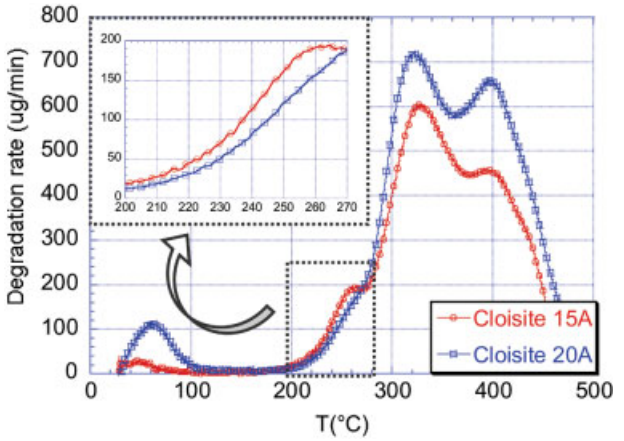

Figure 1 TGA dynamic scans of the nanoclays (in a nitrogen atmosphere). The degradation rate (dm/dt) was plotted as a function of temperature. A detail of the behavior in the temperature range of 200°C–270°C is represented in the upper left box. [Color figure can be viewed in the online issue, which is available at www.interscience.wiley.com.]

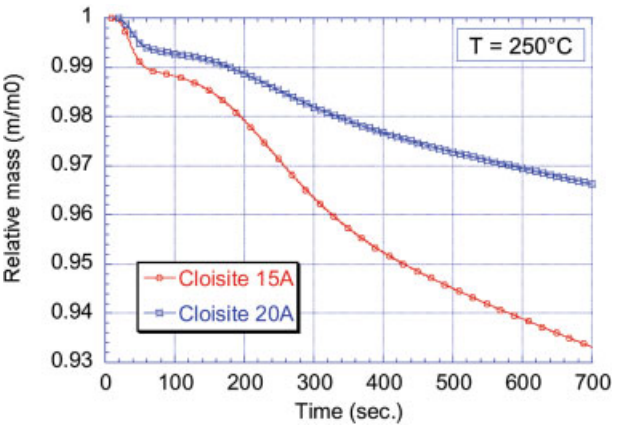

Figure 2 TGA isothermal scans (at 250°C) of the nanoclays (in a nitrogen atmosphere). The relative mass (m/m_0) was plotted as a function of time. [Color figure can be viewed in the online issue, which is available at www.interscience.wiley.com.]

high melting temperature of sPS. It was therefore important and necessary to evaluate the thermal stability of the nanopowders in order to avoid degradation or evaporation of the compatibilizer during processing. Both dynamic (heating from 50°C to 500°C at a rate of 10°C/min) and isothermal tests were performed for each type of Cloisite® preliminarily selected. Figure 1 shows the results of degradation rate versus temperature obtained with a dynamic heating scan in a nitrogen atmosphere. Two main peaks, corresponding to two processes, could be clearly observed. The first peak, at a temperature of around 100°C, could be attributed to first weight loss mainly because of moisture evaporation. Conversely, the second peak (which actually had two parts) resulted from degradation of the organo-modifiers, which in the present study were alkylammonium ions.[6,13,15] Investigating the degradation process was actually beyond the scope of this study, so the only interesting information obtained was on the thermal stability of the nanopowders (closely related to their processing window). In particular, the results of TGA indicated that the Cloisite® 20A was more stable because it had a lower degradation rate in the temperature range of 200°C–300°C, which corresponds to the typical process conditions of aPS and sPS. The results were confirmed by the isothermal tests, shown in Figure 2, performed according to the processing conditions of the polymers studied (to simulate the operating condition of a process such as extrusion or injection molding, the nanoclays were held at 250°C for a relatively long time). Figure 2 shows plots of weight loss versus isothermal holding time. Only a small weight loss (about 2% after 350 s) was observed for Cloisite® 20A, whereas the other reinforcement experienced more significant degradation. Therefore, to produce PS nanocomposites by melt intercalation, the most indicated reinforcement was Cloisite® 20A, as the utilization of less stable compatibilizer would have restricted the gallery between the layers, hindering intercalation of the polymer.

Thermogravimetric tests also were performed on the nanocomposites produced in order to evaluate the effect of the nanofiller on thermal stability and the degradation behavior. Figure 3 shows the weight loss curves, obtained by heating in air four types of samples (pure aPS, pure sPS, sPS/Cloisite® 20A nanocomposite, and aPS/sPS/Cloisite® 20A nanoreinforced blend) from 50°C to 500°C at a rate of 10°C/min. Enhanced thermal stability of the nanoreinforced ma-

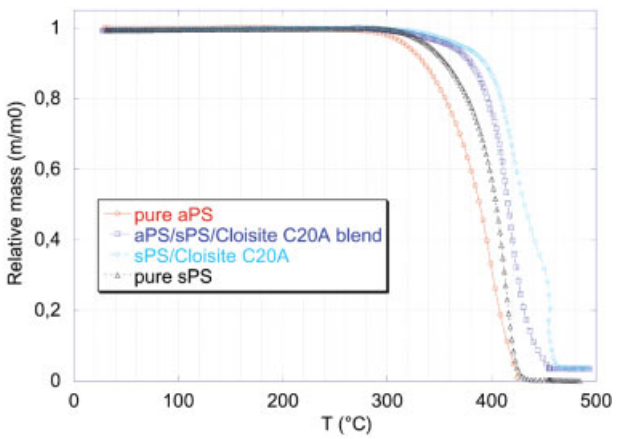

Figure 3 TGA dynamic scans (in air) of both matrices (aPS, sPS) and nanoreinforced materials (sPS-based nanocomposite and aPS/sPS-nanoreinforced blend). Weight loss fraction (m/m_o) was plotted as a function of temperature. [Color figure can be viewed in the online issue, which is available at www.interscience.wiley.com.]

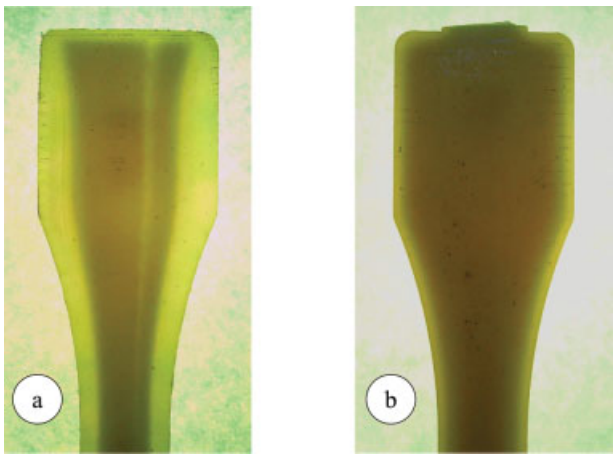

Figure 4 Comparison of pure sPS samples (a) before and (b) after annealing. The amorphous (transparent) phase was replaced by the semicrystalline (matt) phase after thermal treatment. [Color figure can be viewed in the online issue, which is available at www.interscience.wiley.com.]

terials was evident, especially for the sPS/C20A nanocomposite (but also in the aPS/sPS/C20A blend the intercalation of the nanoclay seemed to counterbalance the lower thermal resistance resulting from the presence of aPS). This effect could be ascribed to the barrier effect produced by dispersion of the phyllosilicate within the polymer.[11,16,17]

Wide-angle X-ray diffractometry

Once Cloisite® 20A was chosen to be the reinforcement for the nanocomposites to be analyzed, a set of sPS-based samples was produced by injection molding. These materials then underwent an annealing treatment, which consisted of maintaining the samples at a temperature of 200°C for 2 h and then cooling them slowly to room temperature in order to maximize the fraction of crystalline phase within the polymer matrix. This procedure was necessary in order to obtain materials with nearly uniform characteristics, as injection in a cold mold yielded samples with totally amorphous (transparent) surfaces, as shown in Figure 4.

X-ray diffraction tests were performed in order to check the effective degree of clay dispersion within the polymer. The patterns of both pure sPS and the sPS–Cloisite® 20A nanocomposite in different processing conditions are shown in Figure 5. According to the results of several previous studies,[2,3,5,6,12,18–21] a peak appears at $2\theta = 1.25°–3.75°$ for the composites containing Cloisite®, indicating the presence of an intercalated structure, with a gallery space of about 3.4 nm for the d_{001} reflection (see Table II for further information). The interlayer distance does not seem to depend on the processing conditions, as the annealing process simply lowers the intensity of the corresponding peak. On the other hand, the annealing process favors the

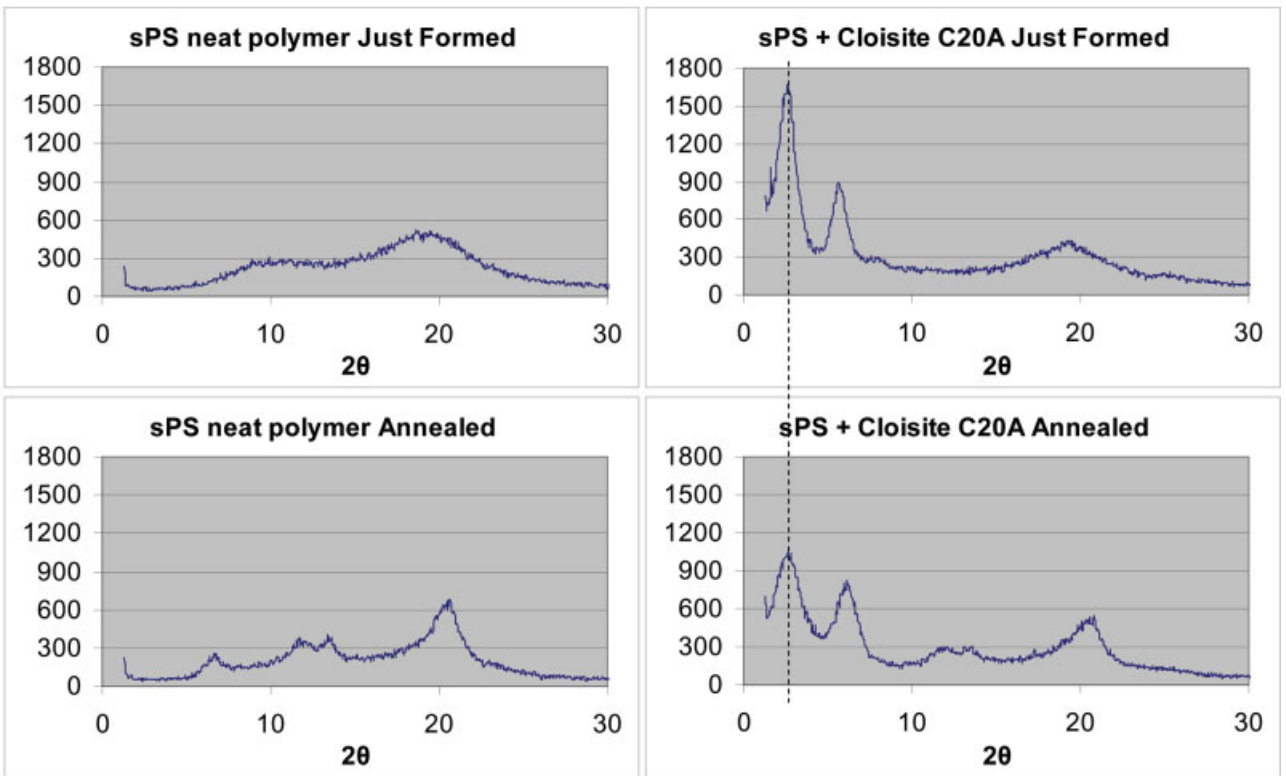

Figure 5 WAXS diffractograms [CuKα radiation: $\lambda = 1.5428$ Å) before and after annealing for both sPS and sPS–Cloisite® 20A nanocomposites. [Color figure can be viewed in the online issue, which is available at www.interscience.wiley.com.]

TABLE II
Nanofiller Gallery Spacing for sPS-Based Nanocomposites

Material	Gallery spacing, d_{001} (nm)
C20A (neat powder) Source: Southern Clay Products, Inc.	2.42
sPS/C20A nanocomposite (Just formed)	3.38
sPS/C20A nanocomposite (after annealing)	3.38

formation of crystalline forms within the polymer, as testified by the appearance of secondary peaks (additional information on identification of the characteristic peaks can be found in refs. 21–24). Note that the crystalline form corresponding to the peak at $2\theta = 5.0°–7.5°$, which also was present in the neat polymer (but only after the annealing process), was strongly enhanced by the presence of the nanofiller, as the peak was present in the nanocomposite even before the annealing process (and did not seem to depend on the thermal history of the material).

Differential Scanning Calorimetry

DSC tests were performed in order to evaluate the effect of the nanocharges and the blending on the thermal properties of the nanocomposites. In the first stage, DSC tests were performed to determine the effect of nanoreinforcement on the glass-transition temperature (T_g) of both the atactic and syndiotactic polymer matrices, because this parameter strongly affects the choice of processing conditions.

The results are shown in Table III. A strong reduction in the T_g was observed only for composites obtained from solution, whereas the composites obtained by melt intercalation showed T_g values approximately equal to that of pure polymer.

These data could be interpreted taking into consideration the state of dispersion of the nanopowder within the polymer: the combined effect of both solutions in toluene and sonication process probably did not favor intercalation of the polymer enough, so Cloisite® particles remained dispersed on a micrometer scale. This produced an increase in the free volume of the polymer, thus lowering the T_g of the nanocomposite materials. Furthermore, a small amount of solvent entrapped in the blend may have plasticized the polymer. On the other hand, in the extrusion process a powerful mechanical mixing at a temperature above the melting point of the polymer seemed to be strong enough to produce its intercalation within the clay galleries. For this reason, the behavior of the nanocomposite materials did not differ so much from that of the pure polymer.

TABLE III
Glass-Transition Temperatures of Analyzed Materials

Material	Forming method	T_g (°C)
Pure aPS		90
aPS/C15A	Intercalation from solution	70
aPS/C20A	Intercalation from solution	65
Pure sPS		95
sPS/C20A	Melt intercalation	93
aPS/sPS/C20A	Melt intercalation	90

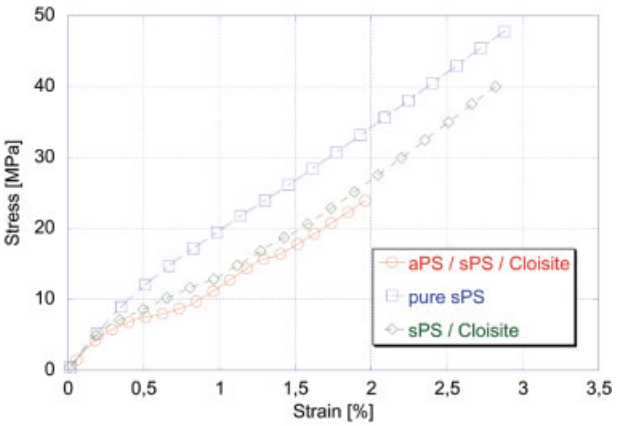

Figure 6 Stress–strain curves of the analyzed materials before annealing. [Color figure can be viewed in the online issue, which is available at www.interscience.wiley.com.]

Mechanical testing

Tensile tests were performed to check whether the dispersion of a nanofiller improvee sPS toughness, thus allowing the use of this polymer in structural applications. Only injection-molded samples were analyzed, as the samples obtained through the intercalation-from-solution method were porous and showed poor characteristics.

A tensile deformation of 5 mm/min [according to UNI-EN ISO 527-2(97) regulations] was first applied to samples not subjected to thermal treatment. Figure 6 shows the results obtained for the three kinds of materials: pure sPS, sPS nanoreinforced with Cloisite® 20A, and the aPS/sPS/C20A nanocomposite blend. It can be seen how the elastic modulus was almost the same for all three materials, whereas the tensile strength and/or elongation at break were appreciably lower for the nanocomposite materials. These results were in agreement with those reported in the literature.[8]

The above-described behavioral changes occurred when the materials were subjected to an annealing treatment. Figures 7 and 8 show the effects of annealing on the pure sPS and the sPS-based nanocomposite, respectively. An expected increase of the Young mod-

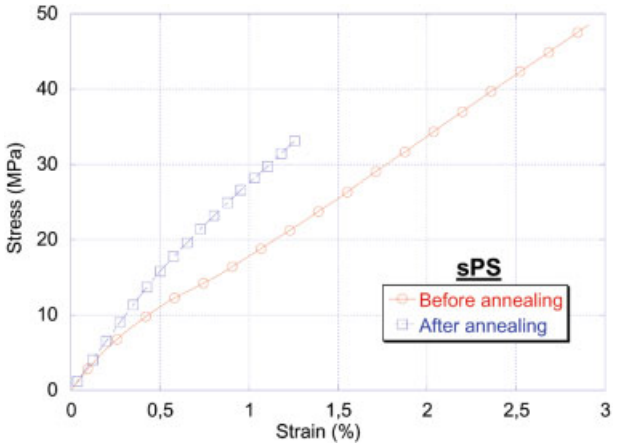

Figure 7 Stress–strain curves of pure sPS before and after annealing. [Color figure can be viewed in the online issue, which is available at www.interscience.wiley.com.]

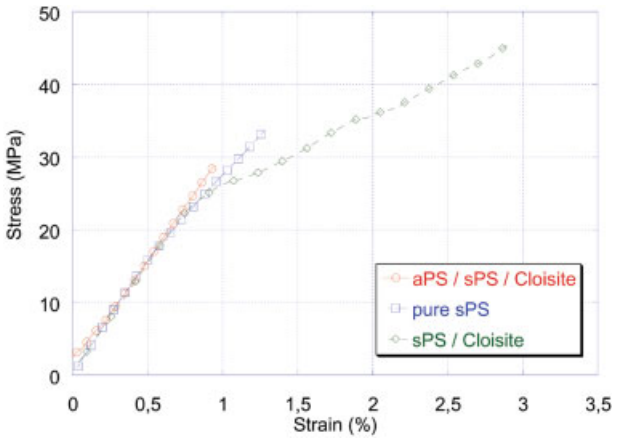

Figure 9 Stress–strain curves of the analyzed materials after annealing. [Color figure can be viewed in the online issue, which is available at www.interscience.wiley.com.]

ulus was observed for in both cases. In the meantime, the mechanical behavior of the neat polymer worsened considerably, whereas the annealed nanocomposite was characterized by a noticeable increase in both stress and elongation at break. As shown in Figure 9, the presence of an intrinsically amorphous phase, such as the blending with aPS, did not compensate for the stiffening of the nanocomposite blend, which behaved like the pure sPS.

Table IV gives a comparison of the performance of the analyzed materials before and after annealing (toughness was calculated as a numerical integration of the stress–strain curve). It must be emphasized that the annealed sPS–based nanocomposite, whose Young modulus, stress at break, and elongation at break were very close to those of the just-formed neat polymer, showed a toughness increase of about 20% and an elongation at break that was double that of the annealed sPS.

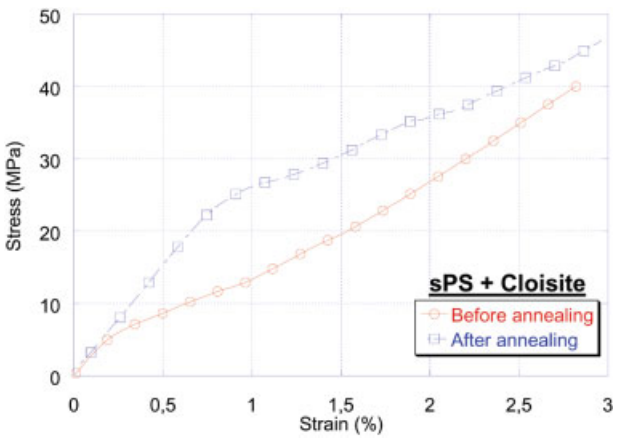

Figure 8 Stress–strain curves of sPS/Cloisite® nanocomposite before and after annealing. [Color figure can be viewed in the online issue, which is available at www.interscience.wiley.com.]

CONCLUSIONS

Thermal and mechanical characterization of three kinds of polystyrene-based materials (pure sPS, sPS/Cloisite® nanocomposite, and aPS/sPS/Cloisite® nanocomposite blend) was performed in order to study the influence of nanoreinforcement and to evaluate its effects on the mechanical and thermal properties. DSC tests showed that the glass-transition temperature of these three materials was strongly dependent on the methodology used to intercalate the nanocharges in the polymer. The T_g decreased when the nanocomposite was obtained through the solution intercalation method, whereas it remained somewhat unchanged after the melt intercalation process. This suggests that the latter method assured there was enough energy to produce clay intercalation, thus lowering the free volume of the polymer.

The TGA test was used to select the most appropriate nanoreinforcement and to evaluate its stability during processing. Furthermore, the thermogravimetric analysis showed enhanced thermal stability of the nanoreinforced materials, which was a result of the barrier effect produced by the dispersion of the phyllosilicate in the polymer.

The X-ray patterns indicated that intercalated structures were obtained in the nanocomposites when Cloisite 20A was used.

Mechanical tests showed that the dispersion of the nanoclay (combined with a proper thermal treatment of the nanocomposite samples) enhanced polymer toughness. Although the presence of intercalated nanoclay seems to be effective in reducing polymer brittleness, the results differed somewhat from the huge increase in mechanical properties obtained with

TABLE IV
Mechanical Properties of Analyzed Materials Before and After Annealing

	sPS	sPS + C20A	aPS + sPS + C20A
Young modulus before annealing (GPa)	3.1	3.2	2.9
Stress at break before annealing (MPa)	46.9	38.3	22.5
Deformation at break before annealing (%)	2.6	2.4	1.6
Young modulus after annealing (GPa)	3.8	3.5	3.4
Stress at break after annealing (MPa)	31.7	43.2	27.8
Deformation at break after annealing (%)	1.2	2.5	0.9
Toughness before annealing (MJ/m^3)	63.5	41.1	16.5
Toughness after annealing (MJ/m^3)	21.1	75.6	13

other polymer-based nanocomposites.[10,11,25] This effect could be ascribed to the lack of clay exfoliation. Therefore, it is clear that improved melt processing is required in order to achieve better exfoliation of the clay, thus widening the range of possible applications of syndiotactic polystyrene.

The authors acknowledge Professor A. M. Maffezzoli of the University of Lecce for useful discussion and suggestions.

References

1. Usuki, A.; Kojima, Y.; Kawasumi, M.; Okada A.; Fukushima, Y.; Kurauchi, T.; Kamigaito, O. J Mat Res 1993, 8, 1179.
2. Wang, D.; Wilkie, C. A. Polym Degrad Stab 2003, 80, 171.
3. Tseng, C. R.; Lee, H. Y.; Chang, F. C. J Polym Sci, Part B: Polym Phys 2001, 39, 2097.
4. Tseng, C. R.; Wu, J. Y.; Lee, H. Y.; Chang, F. C. Polymer 2001, 42, 10063.
5. Park, C. I.; Park, O. O.; Lim J. G.; Kim, H. J. Polymer 2001, 42, 7465.
6. Wang, Z. M.; Chung, T. C.; Gilman, J. W.; Manias, E. J Polym Sci, Part B: Polym Phys 2003, 41, 3173.
7. Wang, J.; Du, J.; Zhu, J.; Wilkie, C. A. Polym Degrad Stab 2002, 77, 249.
8. Zheng, X.; Wilkie, C. A. Polym Degrad Stab 2003, 81, 539.
9. Southern Clay Products, Cloisite Selection Chart Based on Polymer/Monomer Chemistry. Available at: http://www.nanoclay.com/c/c.html
10. Alexandre, M.; Dubois, P. Mater Sci Eng 2000, 28, 1.
11. Gilman, J. W.; Jackson, C. L.; Morgan, A. B.; Harris, R., Jr.; Manias, E.; Giannelis, E. P.; Wuthenow, M.; Hilton, D.; Phillips, S. H. Chem Mater 2000, 12, 1866.
12. Fu, X.; Qutubuddin, S. Mater Lett 2000, 42, 12.
13. Gilman, J. W.; Awad, W. H.; Davis, R. D.; Shields, J.; Harris, R. H.; Davis, C.; Morgan, A. B.; Sutto, T. E.; Callahan, J.; Trulove, P. C.; DeLong, H. C. International Aircraft Fire and Cabin Safety Research Conference, Atlantic City, NJ, 22–25 October, 2001.
14. LeBaron, P. C.; Wang, Z.; Pinnavaia, T. J. Appl Clay Sci 1999, 15, 11.
15. Gilman, J. W.; Bourbigot, S.; Shields, J. R.; Nyden, M.; Kashiwagi, T.; Davis, R. D.; Vanderhart, D. L.; Demory, W.; Wilkie, C. A.; Morgan, A. B.; Harris, J.; Lyon, R. E. J Mater Sci 2003, 38, 4451.
16. Gilman, J. W.; Kashiwagi, T.; Lichtenan, J. D. SAMPE J 1997, 33, 40.
17. Zanetti, M.; Camino, G.; Mulhaupt, R. Polym Degrad Stab 2001, 74, 413.
18. Tanoue, S.; Utracki, L. A.; Garcia-Rejon, A.; Tatibouet, J.; Cole, K. C.; Kamal, M. R. Polym Eng Sci 2004, 44, 1046.
19. Uribe, J.; Kamal, M. R.; Garcia-Rejon, A.; Utracki, L. A. Polymer Processing Society Annual Meeting, Guimarães, Portugal, 2002.
20. Wu, H. D.; Tseng, C. R.; Chang, F. C. Macromolecules 2001, 34, 2992.
21. Wu, T. M.; Hsu, S. F.; Wu, J. Y. J Polym Sci, Part B: Polym Phys 2004, 40, 736.
22. Barnes, J. D.; McKenna, G. B.; Landes, B. G.; Bubeck, R. A.; Bank, D. Polym Eng Sci 1997, 37, 1480.
23. Hodge, K.; Prodpran, T.; Shenogina, N. B.; Nazarenko, S. J Appl Polym Sci 2002, 83, 2705.
24. Wang, C.; Cheng, Y. W.; Hsu, Y. C.; Lin, T. L. J Polym Sci, Part B: Polym Phys 2002, 40, 1626.
25. Nam, P. H.; Maiti, P.; Okamoto, M.; Kotaka, T.; Hasegawa, N.; Usuki, A. Polymer 2001, 42, 9633.